Optical third-harmonic generation in polyacetylene

F. Krausz* and E. Wintner

Abteilung Quantenelektronik und Lasertechnik, Institut für Allgemeine Elektrotechnik und Elektronik, Technische Universität Wien, Gusshausstrasse 27, A-1040 Wien, Austria

G. Leising

Institut für Festkörperphysik, Technische Universität Graz, Petersgasse 16, A-8010 Graz, Austria
(Received 3 August 1988)

Third-harmonic generation experiments have been performed on fully oriented crystalline *trans*-$(CH)_x$ at two laser wavelengths: 1.064 and 1.907 μm. Theoretical analysis of third-harmonic generation in a semiconductor slab is presented which allows the extraction of the electronic third-order susceptibility from the experiments. A simple method was used for the elimination of environmental effects on the measurements. The third-order susceptibilities obtained are $|\chi^{(3)}_{xxxx}(\omega,\omega,\omega)|_{\lambda=1.064\,\mu m}=(9\pm4)\times10^{-9}$ esu and $|\chi^{(3)}_{xxxx}(\omega,\omega,\omega)|_{\lambda=1.907\,\mu m}=(1.7\pm0.7)\times10^{-8}$ esu, representing exceptionally high values compared to other organic and inorganic semiconductors.

I. INTRODUCTION

The fast-growing field of applications of ultrashort light pulses has resulted in great interest in materials having large third-order nonlinear optical coefficients combined with a fast response time. The general nonlinear polarization of a solid-state material arises from the distortion of the nuclear framework and the nonlinear electric response. Whereas the response time of the lattice distortional motion is of the order of tens of femtoseconds, the electric contribution can oscillate at optical frequencies, and therefore may be considered essentially instantaneous in the entire ultrashort time domain. The most straightforward way to determine experimentally the fast electronic response is optical harmonic generation.

The dominant contribution to the polarizability of an electronic system comes quite generally from the electrons in the highest energy levels; the more weakly electrons are bound, the more sensitive they are to perturbations produced by the electromagnetic field. These considerations are clearly mirrored by the fact that semiconductors have nonlinear coefficients by orders of magnitude larger than insulators (Table I). For the same reason, one anticipates a considerable enhancement of the nonlinearity of unsaturated organic molecules (caused by the weakly bound, highly delocalized π electrons) compared to that of the corresponding saturated molecules. Increasing the size of the molecules, the π electron delocalization can get even more pronounced, resulting in further enhancement of the nonlinear coefficients. These ideas have been discussed theoretically and demonstrated experimentally by Ducuing and co-workers.[1-4] To yield large nonlinear polarizations as many molecules as possible should be packed into a unit volume. This condition is only compatible with the above one if the size of the molecules is only large in one direction but small in the other two dimensions. Conjugated polymers, often referred to as one-dimensional (1D) organic semiconductors have all these required properties. Therefore, one expects that a medium consisting of conjugated polymer chains oriented parallel to each other will show strong optical

TABLE I. Optical constants of some organic and inorganic crystals. All $\chi^{(3)}$ values have been measured in the optical gap.

Substance	E_g (eV)	$|\chi^{(3)}_{xxxx}|$ (esu)	$|\chi^{(3)}_{xxxx}|/(\chi^{(1)}_{xx})^4$ (10^{-10} esu)
Quartz	10	3.8×10^{-14}	3.2[a]
β-BaB$_2$O$_4$	6.8	2.3×10^{-13}	6.0[b]
GaAs	1.4	4.8×10^{-11}	1.2[c]
Si	1.1	2.4×10^{-11}	0.5[c]
Ge	0.68	4.0×10^{-10}	2.0[c]
Polydiacetylene (PTS)	2.0	8.5×10^{-10}	5.1×10^{3} [d]
Polyacetylene (*trans*)	1.5	1.7×10^{-8}	390

[a]Reference 20.
[b]Reference 30.
[c]Reference 31.
[d]Reference 5.

nonlinearity. The highest chain density can be produced in the solid phase. Following the above ideas, third-harmonic generation (THG) measurements[5] on bulk polydiacetylene, which was the first one-dimensional organic semiconductor crystal, have yielded very large values of the electronic $\chi^{(3)}$ comparable to those of inorganic semiconductors ($\sim 10^{-10}$ esu).

In recent years much interest has been focused on polyacetylene $(CH)_x$, which is the most simple conjugated polymer and thus is referred to as the prototype 1D organic semiconductor (Fig. 1). For a long time $(CH)_x$ samples have almost exclusively been prepared by the so-called Shirakawa technique.[6] Such samples show neither single crystal nor polycrystalline morphology but consist of irregularly arranged partially crystalline fibers, and contain considerable amounts of empty space between them. Such a complex morphology caused a variety of problems in both what concerns the measurement of the optical properties and also their physical interpretation. With respect to the nonlinear properties the orientational averaging as well as the low density significantly reduce the third-order susceptibility. Nevertheless, recent THG measurements[7,8] on $(CH)_x$ samples of this kind gave $\chi^{(3)}$ values in excess of 10^{-10} esu. These results suggest a very large intrinsic electronic nonlinearity of the polyacetylene chains.

Recently, one of us (G.L.) has succeeded in developing a method to prepare fully oriented crystalline polyacetylene, utilizing a precursor polymer[9] which is converted to polyacetylene under applied stress.[10] 100% trans-$(CH)_x$ films can be obtained in this way with thicknesses ranging from about 0.2 μm up to several micrometers. The material exhibits a compact, nonfibrous, dense morphology and smooth surfaces as revealed by scanning electron microscopy. The bulk density has a value of 1.1 g/cm^3, which is close to the theoretical x-ray density of 1.2 g/cm^3, and about a factor of 3 higher than the density of $(CH)_x$ films prepared by the Shirakawa method. X-ray diffraction and high-energy electron diffraction measurements evidence a nearly perfect alignment of the polymer chains parallel to the stretching direction. The unit cell was found to be monoclinic with the space group $P2_1/a$.[11] The homogeneous bulk and the high quality surfaces allowed reliable determination of the linear anisotropic optical constants of the material by polarized

FIG. 1. Structure of trans-$(CH)_x$. u_0 denotes the amplitude of the Peierls distortion. $2a$ is the length of the elementary cell of the chain (one-dimensional solid).

optical reflectivity measurements.[12] This is indispensable for the evaluation of nonlinear optical measurements.

We carried out THG measurements on such crystalline trans-$(CH)_x$ samples for the first time. Care has to be taken when evaluating the measured data. In general, in a plane-parallel slab the reflected as well as the forward propagating fundamental waves generate nonlinear polarization. Whereas in insulating optical crystals the dispersion of the linear optical constants is usually small and thus, as we shall see in Sec. II, the contribution to the nonlinear polarization generated by the reflected fundamental can be neglected; this is not the case in semiconductors. The large values of the linear optical constants and their characteristic strong dispersion around the gap may lead to an uncommon situation in semiconductors: two or more harmonic waves with different wave vectors but the same frequency resulting from the mixing of the forward propagating and reflected fundamental waves may have amplitudes of the same order of magnitude. The transmitted and reflected third-harmonic (TH) waves, which can be detected result from the interference of these waves.

In Sec. II, recalling some fundamental equations describing harmonic wave generation and propagation in a nonlinear medium, we will discuss optical third-harmonic generation in a semiconductor slab in detail. The experimental design for measurement of the third-order susceptibility of a thin semiconductor sample is described in Sec. III. In Sec. IV the experimental results are presented and discussed. Finally, conclusions are drawn in Sec. V.

II. THEORY

Optical wave propagation in the nonlinear (NL) media has been described by Bloembergen et al.[13,14] Waves at the third-harmonic frequency are governed by the equation

$$\nabla \times \nabla \times \mathbf{E}^{3\omega} + \frac{\varepsilon(3\omega)}{c^2} \frac{\partial^2 \mathbf{E}^{3\omega}}{\partial t^2} = -\frac{4\pi}{c^2} \frac{\partial^2 \mathbf{P}_{NL}^{3\omega}}{\partial t^2} . \quad (1)$$

In the small conversion approximation the fundamental waves obey the homogeneous wave equation, and the source term in Eq. (1) is determined by the fundamental waves, which are unaffected by the nonlinear polarization.

For the present problem, we restrict ourselves to the special case of third-harmonic generation in a nonlinear slab when all the electric field strengths are polarized parallel to the x axis (see Fig. 2), which is supposed to coincide with an optical axis of the nonlinear medium. Then in scalar formalism, using the infinite plane-wave approximation,

$$E_l^\omega(\mathbf{r}, t) = A_l^\omega \exp[i(\mathbf{k}_l^\omega \cdot \mathbf{r} - \omega t)] . \quad (2a)$$

$l = 1$ denotes the incident fundamental wave and $l: f, b, r, t$ refer to free (homogeneous) waves shown in Fig. 2.[15] The nonlinear polarization oscillating at the third-harmonic frequency is as follows:[16]
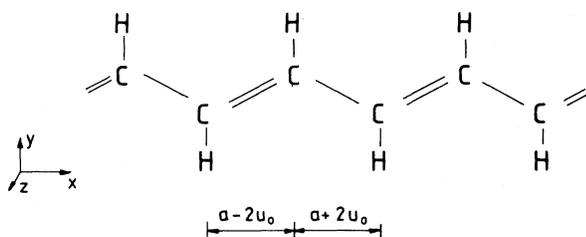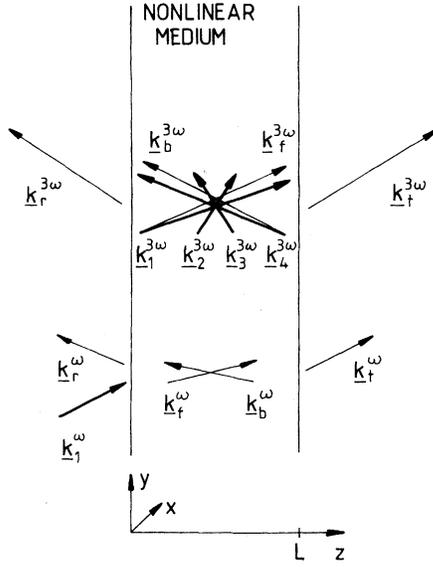
NONLINEAR
MEDIUM

FIG. 2. Waves in the nonlinear plane parallel slab. Fundamental waves with wave vectors $\mathbf{k}_f^\omega, \mathbf{k}_b^\omega$ give rise to inhomogeneous waves at 3ω with wave vectors $\mathbf{k}_1^{3\omega}$, $\mathbf{k}_2^{3\omega}$, $\mathbf{k}_3^{3\omega}$, and $\mathbf{k}_4^{3\omega}$. Thin arrows denote the wave vectors of the homogeneous waves.

$$P_{\mathrm{NL}}^{3\omega}(\mathbf{r},t)=\chi_{xxxx}^{(3)}(\omega,\omega,\omega)\sum_{j=1}^{4} E_f^\omega(\mathbf{r},t)^{4-j}E_b^\omega(\mathbf{r},t)^{j-1} \ . \qquad (3)$$

This polarization creates electric fields oscillating at the third-harmonic frequency:

$$E_l^{3\omega}(\mathbf{r},t)= A_l^{3\omega}\exp[i\,(\mathbf{k}_l^{3\omega}\cdot\mathbf{r}-3\omega t)] \ . \qquad (2b)$$

In our notation, the subscript l is replaced by numbers $j=1,2,3,4$ for driven (inhomogeneous) harmonic waves, which are the solutions of the inhomogeneous wave equation, whereas $l:f,b,r,t$ stand for the solutions of the homogeneous wave equation, which are needed to fulfill the boundary conditions (Fig. 2).

The absolute values of the corresponding wave vectors at ω are

$$k_1^\omega=k_r^\omega=\epsilon'(\omega)^{1/2}(\omega/c), \quad k_t^\omega=\epsilon''(\omega)^{1/2}(\omega/c)$$

$$k_f^\omega=k_b^\omega=\epsilon_{xx}(\omega)^{1/2}(\omega/c) \qquad (4)$$

and the directions are fixed by the boundary conditions at the intersections of the nonlinear and linear media:

$$k_{ly}^\omega=k_{1y}^\omega=k_1^\omega\sin\theta, \quad k_{lz}^\omega=[(k_l^\omega)^2-(k_{ly}^\omega)^2]^{1/2} \ , \qquad (5)$$

where θ is the angle of incidence of the fundamental wave, ϵ' and ϵ'' denote the dielectric constants of the surrounding isotropic linear media, and ϵ_{xx} is the corresponding element of the dielectric tensor of the nonlinear medium. All of the dielectric constants might be complex in a general case.

Presuming the fundamental optical pulse to be much longer than the thickness L of the nonlinear medium, the amplitudes A_f^ω and A_b^ω (depending consequently only on the time) are given by the following relations:

$$A_f^\omega=fA_1^\omega \ , \qquad (6a)$$

$$A_b^\omega=bA_1^\omega \ , \qquad (6b)$$

$$f=\frac{2k_{1z}^\omega}{(k_{1z}^\omega+k_{fz}^\omega)+\exp(2ik_{fz}^\omega L)(k_{fz}^\omega-k_{1z}^\omega)(k_{fz}^\omega-k_{tz}^\omega)/(k_{fz}^\omega+k_{tz}^\omega)} \ , \qquad (7a)$$

$$b=f\,\exp(2ik_{fz}^\omega L)(k_{fz}^\omega-k_{tz}^\omega)/(k_{fz}^\omega+k_{tz}^\omega) \ . \qquad (7b)$$

The four inhomogenous harmonic waves resulting from the mixing of these two fundamental waves are

$$E_j^{3\omega}(\mathbf{r},t)= A_j^{3\omega}\exp[i\,(\mathbf{k}_j^{3\omega}\cdot\mathbf{r}-3\omega t)] \ , \qquad (8)$$

where

$$A_j^{3\omega}=\frac{4\pi\chi_{xxxx}^{(3)}(\omega,\omega,\omega)}{\epsilon_{xx}(3\omega)}\frac{(k_f^{3\omega})^2}{(k_j^{3\omega})^2-(k_f^{3\omega})^2}(A_f^\omega)^{4-j}(A_b^\omega)^{j-1} \ , \qquad (9)$$

and

$$\mathbf{k}_j^{3\omega}=(4-j)\mathbf{k}_f^\omega+(j-1)\mathbf{k}_b^\omega, \quad j=1,2,3,4 \ . \qquad (10)$$

Again, the wave vectors and amplitudes of the free harmonic waves can be determined from the boundary conditions. With

$$k_r^{3\omega}=\epsilon'(3\omega)^{1/2}(3\omega/c), \quad k_t^{3\omega}=\epsilon''(3\omega)^{1/2}(3\omega/c), \quad k_f^{3\omega}=k_b^{3\omega}=\epsilon_{xx}(3\omega)^{1/2}(3\omega/c) \ , \qquad (11)$$

the y components are

$$k_{ly}^{3\omega}=k_{jy}^{3\omega}=3k_1^\omega\sin\theta \ . \qquad (12)$$

From an experimental point of view, we are interested in the free waves propagating outside the nonlinear medium. Their amplitudes can be expressed as the linear combination of those of the driven waves:

$$A_t^{3\omega} = \sum_{j=1}^{4} t_j A_j^{3\omega} , \tag{13a}$$

$$A_r^{3\omega} = \sum_{j=1}^{4} r_j A_j^{3\omega} . \tag{13b}$$

The transmission and reflection factors are

$$t_j = \frac{2(\Delta k_r - \Delta k_j) + a_j a_f \Delta k_j (2 - \Delta k_r / k) - a_j a_f^{-1} \Delta k_r (2 - \Delta k_j / k)}{a_t a_f \Delta k_t (2 - \Delta k_r / k) - a_t a_f^{-1} \Delta k_r (2 - \Delta k_t / k)} , \tag{14a}$$

and

$$r_j = \frac{2a_j(\Delta k_t - \Delta k_j) + a_f^{-1} \Delta k_j (2 - \Delta k_t / k) - a_f \Delta k_t (2 - \Delta k_j / k)}{a_f^{-1} \Delta k_r (2 - \Delta k_t / k) - a_f \Delta k_t (2 - \Delta k_r / k)} , \tag{14b}$$

where $\Delta k_j = k_{fz}^{3\omega} - k_{jz}^{3\omega}$, $\Delta k_r = k_{fz}^{3\omega} - k_{rz}^{3\omega}$, $\Delta k_t = k_{fz}^{3\omega} - k_{tz}^{3\omega}$, and $k = k_{fz}^{3\omega}$. Furthermore, $a_f = \exp(ik_{fz}^{3\omega}L)$, $a_j = \exp(ik_{jz}^{3\omega}L)$, and $a_t = \exp(ik_{tz}^{3\omega}L)$.

In deriving the above formulas needed for the evaluation of THG measurements, we have made some basic approximations, such as the small conversion approximation and the infinite plane-wave approximation. While the former is a very good approximation unless high efficiency phase-matched harmonic generation or parametric amplification is considered, the latter is valid only if the waist of the incident laser beam is much larger than the wavelength, the sample thickness is much less than the confocal parameter of the focused Gaussian beam, and $L \sin\theta \ll 2w_0$ (w_0 is the beam waist). Furthermore, if the laser pulse is not bandwidth limited, the assumption of a perfectly coherent fundamental wave in our calculations may also lead to errors in the interpretation of the experimental data.[17] We shall overcome this problem by utilizing a reference method for the measurement of the nonlinear coefficient. We did not make use of the slowly varying amplitude approximation because it breaks down whenever the dispersion of the linear constants becomes appreciable.

The above concepts can be followed to derive similar expressions for other polarization directions, and the formulas are not much more complicated until the plane of incidence contains two optical axes of the nonlinear medium. In the case of nonvanishing $\chi^{(2)}$ cascading processes must also be included in the theory.

Employing our results for optical crystals showing a small dispersion from (9) follows that $A_1^{3\omega} \gg A_j^{3\omega}$ for $j = 2, 3, 4$, which is the consequence of the small dispersion:

$$(k_f^{3\omega})^2 - (k_1^{3\omega})^2 \ll (k_f^{3\omega})^2 - (k_j^{3\omega})^2 , \quad j = 2, 3 \tag{15}$$

and of the moderate values of the linear constants: $A_b^{\omega} \ll A_f^{\omega}$. Taking into account these considerations and supposing $\epsilon' = \epsilon'' = 1$, the amplitude of the transmitted third-harmonic wave is found from Eqs. (6a), (7a), (9), (13a), and (14a) as

$$A_t^{3\omega} = \frac{4\pi\chi_{xxxx}^{(3)}(\omega,\omega,\omega)}{\epsilon_{xx}(\omega) - \epsilon_{xx}(3\omega)} T(\theta)\{1 - \exp[i\Delta\phi(\theta)]\}(A_1^{\omega})^3 , \tag{16}$$

where

$$T(\theta) = \frac{2[\epsilon_{xx}(3\omega) - \sin^2\theta]^{1/2}}{[\epsilon_{xx}(3\omega) - \sin^2\theta]^{1/2} + \cos\theta}$$
$$\times \left[\frac{2\cos\theta}{[\epsilon_{xx}(\omega) - \sin^2\theta]^{1/2} + \cos\theta} \right]^3 \tag{17}$$

and

$$\Delta\phi(\theta) = 3k_1^{\omega}\{[\epsilon_{xx}(3\omega) - \sin^2\theta]^{1/2}$$
$$- [\epsilon_{xx}(\omega) - \sin^2\theta]^{1/2}\}L . \tag{18}$$

For the reflected wave

$$|A_r^{3\omega}/A_t^{3\omega}| = |r_1/t_1| = \Delta k_t/\Delta k_r \tag{19}$$

which (again due to the moderate value of the dielectric constant) is considerably smaller than unity.

In a semiconductor, for a fundamental wave of photon energy lower than the band gap, A_b^{ω} may be comparable to A_f^{ω} owing to the large dielectric constant of the semiconductor crystal. Additionally, in semiconductors the dispersion is known to be strong in a rather broad wavelength region around the band gap. Therefore (15) might be invalid. As a result, two or more driven third-harmonic waves may have comparable amplitudes, thus the reflected and transmitted third-harmonic waves result from the interference of these driven waves. Interference of waves generated by the nonlinear polarization has been reported by several authors,[18-20] where the interfering waves originated from different contributions to the nonlinear polarization, such as Raman nonlinearity and electronic nonlinearity, or second-order and third-order electronic nonlinearity. In our case, however, the interference results from the mixing of *different* fundamental waves by the *same* nonlinear susceptibility.

In polyacetylene, owing to the extremely large disper-

sion of ϵ, the interference between driven harmonic waves is expected to be pronounced. Taking the values of ϵ of trans-$(CH)_x$ for the fundamental wavelength $\lambda = 1.064$ μm and for the corresponding third harmonic to be $\epsilon_{xx}(\omega) = 16.4 + 1.79i$, and $\epsilon_{xx}(3\omega) = -1.20 + 1.24i$, respectively, we derive $n(\omega) = 4.06$, $\alpha(\omega) = 2.60 \times 10^4$ cm^{-1}; $n(3\omega) = 0.513$, $\alpha(3\omega) = 4.28 \times 10^5$ cm^{-1}, where n and α denote the real refractive index and the absorption coefficient, respectively. If the sample thickness is much greater than the absorption length for the third harmonic, i.e., $\alpha(3\omega)L \gg 1$, then $a_f \ll 1$, and to a good approximation

$$t_j = \frac{k_{fz}^{3\omega} + k_{jz}^{3\omega}}{k_{fz}^{3\omega} + k_{tz}^{3\omega}} \exp(ik_{jz}^{3\omega}L) \; , \tag{20a}$$

$$r_j = \frac{k_{fz}^{3\omega} - k_{jz}^{3\omega}}{k_{fz}^{3\omega} - k_{rz}^{3\omega}} \; , \tag{20b}$$

where the phase factor a_t^{-1} has been omitted from (20a). Using these formulas and the numerical values of the linear optical constants, we can calculate the dependence of the intensity of the transmitted harmonic wave on the sample thickness. The results of these calculations are plotted in Fig. 3 for normal incidence. The local maxima and minima result from the interference of driven third-harmonic waves inside the slab, whereas the overall decay of the transmitted signal is due to the absorption of the fundamental beam. It is worth emphasizing that the TH intensity dependence in Fig. 3 has nothing to do with the intensity fringes originating from nonphase-matched harmonic generation in an insulating crystal where they are the result of interference of a free and a driven wave. From the periodicity of $I_t^{3\omega}$ we can see that the dominant waves contributing to this pattern shown in Fig. 3 are $E_1^{3\omega}$ and $E_2^{3\omega}$. As expected, the interference fringes begin to disappear as L becomes reasonably larger than the absorption length at the fundamental wavelength. The reason for this behavior is the vanishing A_b^ω according to
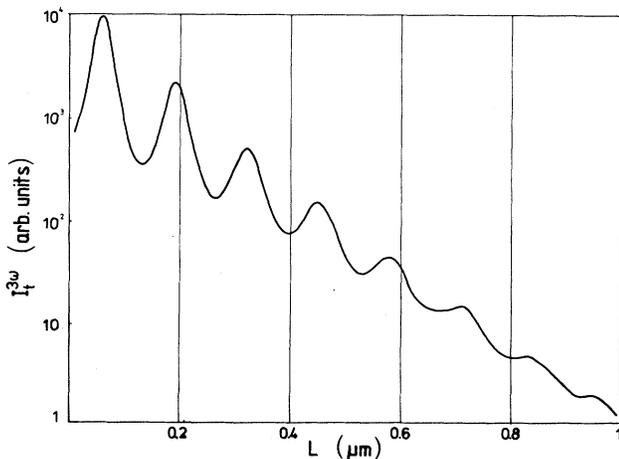
FIG. 3. Intensity of the transmitted third-harmonic wave as a function of the sample thickness for constant pump intensity at $\lambda_\omega = 1.064$ μm and $\theta = 0$ incident angle.
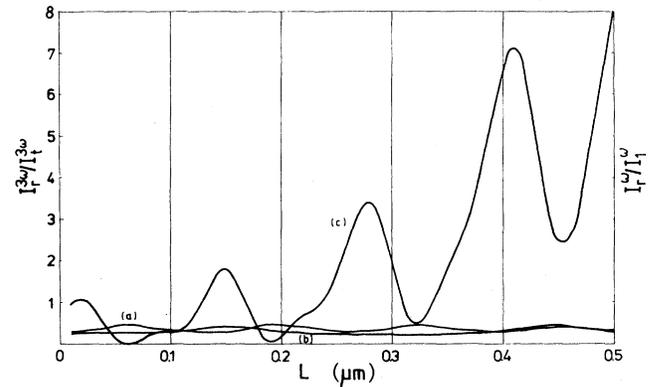
FIG. 4. Ratio of the reflected and transmitted third-harmonic intensities (c) and the reflected and incident fundamental intensities [(a) and (b)] as a function of the sample thickness under the same conditions as in Figs. 3(a)–3(c) are calculated for $\lambda_\omega = 1$, 2, and 1.064 μm, respectively.

(7b). In a region of $L < 1/\alpha(\omega)$, however, $I_t^{3\omega}$ is a sensitive function of L, due to the pronounced interference of the driven harmonics in the plane parallel slab. The variation of $I_r^{3\omega}$ with respect to L is much slower, owing to the lack of the phase factor $\exp(ik_{jz}^{3\omega}L)$ in (20b). The ratio of $I_r^{3\omega}$ and $I_t^{3\omega}$, which is independent of $\chi^{(3)}$ and the pump intensity, is shown in Fig. 4. The ratio I_r^ω/I_1^ω is also plotted in Fig. 4 for later reference.

III. EXPERIMENTS

A. Experimental setup

We have performed optical third-harmonic generation measurements on oriented crystalline trans-$(CH)_x$ samples at fundamental wavelengths of 1.064 and 1.907 μm. The experimental arrangement used to generate and detect the third harmonic is shown in Fig. 5. The light source is a Q-switched Nd:YAG (yttrium aluminum garnet) laser delivering pulses of about 10-ns duration of a repetition rate of 10 pps at 1.064 μm wavelength. The fundamental beam at 1.907 μm was created in a pressurized ($p = 40$ bar) hydrogen gas Raman-cell by single Stokes shifting the laser light. Glan-Thomson polarizers were employed to fix the polarization of the fundamental beam, which was selected by filters F_1–F_3. A 10% single surface reflection was split off prior to the lenses focusing the beam onto the sample, and was used to produce a third-harmonic signal in a silica plate for pulse-by-pulse normalization against possible fluctuations of the coherence properties[17] as well as the energy of the fundamental pulses.

The sample arm was designed to allow a perfectly symmetric detection of the reflected and transmitted third harmonics. For this reason a negative lens L_3 and two dichroic mirrors transparent for ω and reflective for 3ω were used in addition to the focusing lenses L_4. The arrangement also results in a small confocal parameter of the focused fundamental beam, the significance of which will be discussed later. The signals for the photomulti-
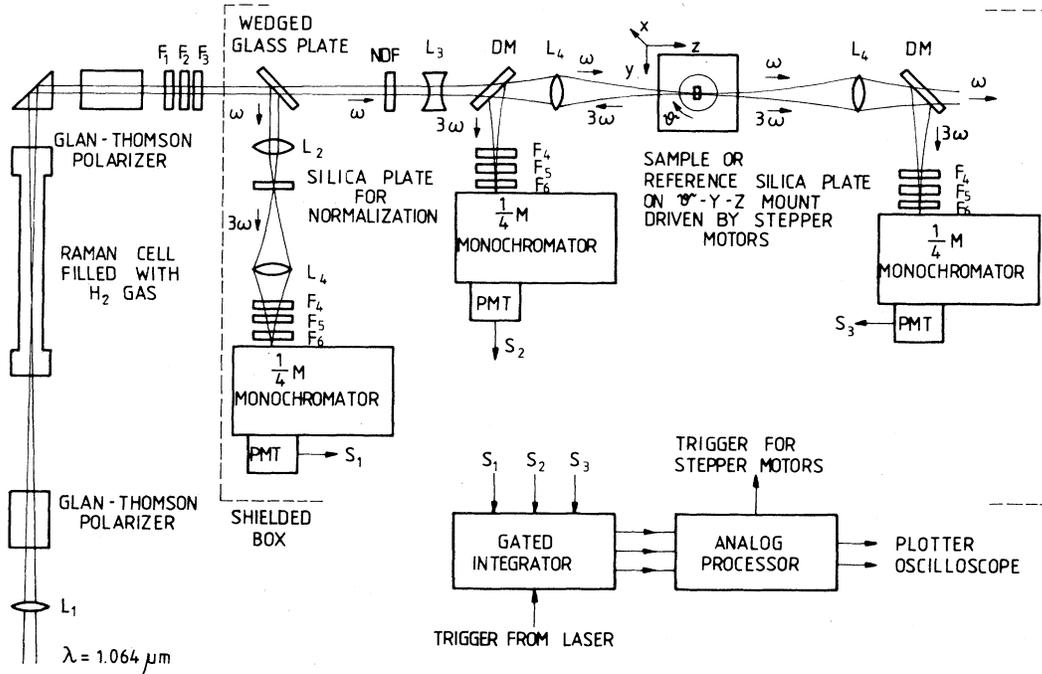
FIG. 5. Experimental apparatus for third-harmonic generation measurements. L_1-L_4, lenses with $f_1 = 1000$ mm, $f_2 = 50$ mm, $f_3 = -30$ mm, and $f_4 = 75$ mm, respectively; F_1-F_3, optical filters for selecting the desired fundamental beam at ω; F_4-F_6, filters for isolation of the third harmonic at 3ω; NDF, neutral density filter; DM, dichroic mirrors; PMT, photomultiplier tubes with S20 photocathode.

pliers were integrated by boxcar integrators. Signals S_2 and S_3 were subsequently divided by S_1 in an analog processor. The residual noise was subtracted from the total output of each channel before taking the ratio of the outputs. Single fluctuations of the normalized signals were suppressed by a filter with a time constant of $\tau = 0.3$ s. Finally, the normalized outputs S_2/S_1 and S_3/S_1 were plotted.

B. Environmental effects

Because of the finite value of $\chi^{(3)}$ of air we have to be concerned with its influence on THG experiments. The reason why this effect must be taken into account despite the very small value of $\chi^{(3)}$ of the atmospheric air can be seen from formula (16). Actually, the generated third harmonic is proportional not only to $\chi^{(3)}$ but also to $1/[\epsilon(3\omega) - \epsilon(\omega)]$. For the sake of simplicity we drop here the subscripts of ϵ and $\chi^{(3)}$. In the case of small absorption, it makes physical sense to introduce the coherence length of harmonic generation. It can be defined by the path length along which the created harmonic fields add up constructively. Setting $\theta = 0$ in Eq. (18) we immediately get for THG $l_c = \lambda_\omega/6|n(3\omega) - n(\omega)|$, where λ_ω denotes the fundamental wavelength. For small dispersion straightforward algebra yields: $\chi^{(3)}/|\epsilon(3\omega) - \epsilon(\omega)| = 3\chi^{(3)}l_c/n\lambda_\omega$. As a consequence, under non-phase-matched conditions the generated third-harmonic intensity is proportional to the square of $|\chi^{(3)}|l_c/n$. Although these considerations are based on our results de-

rived for THG in a finite slab, it can be shown that formulas (16) and (18) describe THG by a plane wave also in an infinite medium like air provided that the substitutions $\theta = 0$, $T = 1$, and $L \to z$ are performed. Then, we are able to compare the orders of magnitudes of the third-harmonic powers created by the same fundamental beam in air and, for example, in a silica slab.

Taking for air[21-24] and silica[25,26] at $\lambda_\omega = 1.064$ μm for the following values:

$$[n(3\omega) - n(\omega)]_A = 1.09 \times 10^{-5} \ .$$

$$|\chi^{(3)}|_A = 3.2 \times 10^{-18} \text{ esu} \ ,$$

$$[n(3\omega) - n(\omega)]_S = 2.65 \times 10^{-2} \ .$$

$$|\chi^{(3)}|_S = 3.1 \times 10^{-14} \text{ esu} \ ,$$

we get the coherence lengths

$$(l_c)_A = 16.3 \text{ mm}$$

and

$$(l_c)_S = 6.69 \ \mu\text{m} \ .$$

The parameters governing THG under nonindex-matched conditions are

$$|\chi^{(3)}l_c/n|_A = 5.2 \times 10^{-18} \text{ esu} \ ,$$

$$|\chi^{(3)}l_c/n|_S = 1.4 \times 10^{-17} \text{ esu} \ .$$

If harmonic fields created in air on both sides of the slab added oppositely to the harmonic field created in the slab, they might yield an order-of-magnitude reduction of the silica plate signal according to our estimation.

In fact, a factor of 4 change in intensity of THG fringe patterns has been observed when the air surrounding a silica plate was removed.[26,27] Therefore, the conclusion was drawn that THG experiments on optical materials with relatively small nonlinear constants ($\chi^{(3)} \sim 10^{-14}$ -10^{-13} esu) should be done in vacuum, in order to extract correct $\chi^{(3)}$ coefficients from the measured data. The problem of the surrounding air exists in almost all reference THG measurements, because the most suitable reference materials for the calibration of nonlinear susceptibilities are those having a broad transparency region and nearly constant nonlinear coefficients, such as quartz, silica, and soft glasses, all of which have $\chi^{(3)}$ values of the order of $10^{-14}-10^{-13}$ esu.

However, the use of a vacuum chamber may lead to difficulties in some cases. Therefore, we propose a very simple way to get rid of the disturbing influence of air on THG measurements. Our above considerations apply for the case when the confocal parameter of the fundamental beam is much larger than the coherence length in air: $b \gg (l_c)_A$. Otherwise, if $b < (l_c)_A$, l_c should be replaced by b in the estimation of the air contribution to the resultant TH signal. As a result, by sufficiently tight focusing, the air contribution can be suppressed. Taking $b/(l_c)_A = 0.1$, the influence of air on the intensity of the harmonic field created in the silica slab should be smaller than 10%.

To verify these findings experimentally, we performed some preliminary THG measurements on a silica plate placed in the center of a 25-cm long optical vacuum cell with fundamental beams of different confocal lengths. Then, the experiments were repeated in atmospheric environment. The comparison yielded reductions of the silica plate signals in air of a factor of about 3 and less than 10% for $b_1 = 76$ and $b_2 = 1.8$ mm, respectively. These results are in reasonable agreement with our rough estimates. A more rigorous study of the influence of air on THG experiments will be presented elsewhere.[28]

The confocal parameter of the fundamental beam in the arrangement of Fig. 5 is $b = 1.8$ mm. This small value of b reduces the error of the measurement of $\chi^{(3)}$ caused by the surrounding air to below 5%, which is negligible compared to the other experimental errors, but still allows the use of the infinite plane-wave approximation in the evaluation of the measurements for reasonable sample thicknesses ($L \lesssim 1$ mm). Also, the beam diameter remains large enough ($d \sim 50$ μm) to produce sufficient third-harmonic signals for detection.

C. Experimental procedure

First,[29] we placed the calibration silica plate of a thickness of ~ 0.2 mm on the translation-rotation stage shown in Fig. 5. The plate was positioned with the center at the beam waist, and rotated along a vertical axis parallel to the incident beam polarization. The normalized third-harmonic output from the calibration plate $(S_3/S_1)_{cal}$ is

depicted in Fig. 6 for two different values of the confocal parameter of the fundamental beam. With the free parameters A_1^{φ} and L, the excellent agreement of a least-squares fit of Eq. (16) to the experimental points in Fig. 6 for $b = 1.8$ mm confirms that the influence of air on the TH intensity is negligible in this situation. However, in the case of $b = 76$ mm the peaks of the Maker fringes decrease much faster with increasing θ than predicted by Eq. (16). This is clearly the consequence of the air contribution to the harmonic field created by the plate. The error bar indicates a relatively small experimental uncertainty, owing to the pulse-by-pulse normalization technique.

The trans-$(CH)_x$ sample was prepared on a silica substrate and held in an inert atmosphere in a Suprasil optical cuvette. The sample thickness was determined by polarized reflectivity measurements in a wavelength range well above the band gap yielding a value of $L = (0.35 \pm 0.02)$ μm. Additionally, the results of Sec. II allow us to obtain a more accurate value of L at the same location where the $\chi^{(3)}$ measurement is performed. In fact, according to Fig. 4 the ratio of $I_r^{3\omega}$ and $I_t^{3\omega}$ yields the sample thickness directly, provided that we know it with an accuracy corresponding to a region where $I_r^{3\omega}/I_t^{3\omega}$ is a unique function of L. The sample was also positioned at the fundamental beam waist with chain direction parallel to the x axis. The incident beam was also polarized in this direction. Setting $\theta = 0$, moving the sample transversely along the y axis (see Fig. 5) and dividing S_2 by S_3 in the analog processor we measured $I_r^{3\omega}/I_t^{3\omega}$ at $\lambda_\omega = 1.064$ μm. Making use of Fig. 4, the evaluated thickness is plotted in Fig. 7 as a function of y for two different x coordinates with a spacing of about 1 mm between them. As expected, the curves reveal a clear correlation along the chain direction. The strong variations of the ratio $I_r^{3\omega}/I_t^{3\omega}$ along the y direction correlating for different x coordinates are indirect evidence for the interference phenomenon discussed earlier.
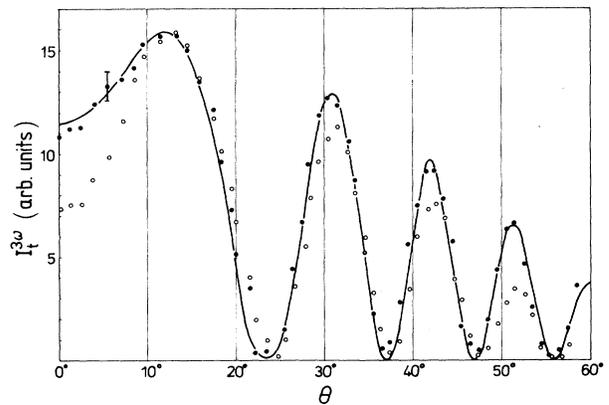
FIG. 6. Variation of the third-harmonic intensity with the angle of rotation about a vertical axis parallel to the fundamental beam polarization. ●, experimental results for $b = 1.8$ mm; ○, experimental results for $b = 76$ mm; the solid curve is the theoretical variation from Eq. (16).
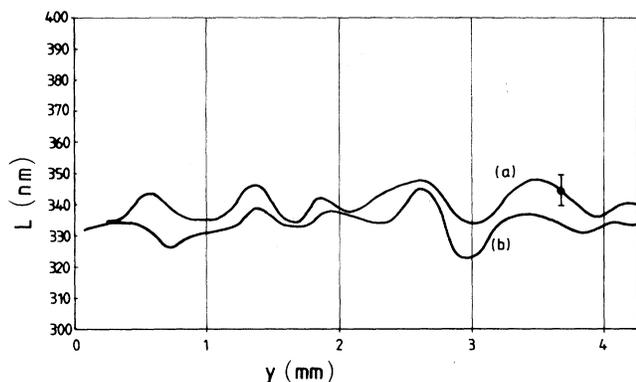
FIG. 7. Thickness variation of the sample evaluated from the variation of the ratio of the reflected and transmitted third-harmonic signals along the y direction. Curves (a) and (b) were measured at different x coordinates in a distance of about 1 mm of each other.

For comparison, we have also depicted I_r^ω/I_t^ω in Fig. 4 for two fundamental wavelengths at which the sample is transparent. It is apparent that our nonlinear interference method assures an order-of-magnitude greater accuracy than the commonly used linear interference technique. This is generally true for any sample thickness. The thicker the sample is the longer wavelength must be used in both measurements to satisfy the condition $\alpha(\omega)L \ll 1$. The small fluctuations of the ratio $I_r^{3\omega}/I_t^{3\omega}$ would allow the determination of L with an accuracy of about 2 nm in our case. However, the precision is limited by the accuracy of the linear optical constants, as indicated by the error bar in Fig. 7.

Now, measuring S_2/S_1 and S_3/S_1 at $\theta=0$ and with a fundamental beam polarized parallel to the x axis, knowing L and the linear optical constants we are able to extract $|\chi_{xxxx}^{(3)}(\omega,\omega,\omega)|_{(CH)_x}/|\chi^{(3)}(\omega,\omega,\omega)|_{silica}$ from the measurements. The dynamic range of the relative measurement was extended by using calibrated neutral-density filters (NDF) to attenuate the fundamental beam prior to the sample. We take for silica $|\chi^{(3)}(\omega,\omega,\omega)|$ $=2.8\times10^{-14}$ esu measured by Meredith et al. at 1.907 μm. In order to have a calibration value also at 1.064 μm the generalized Miller's rule $\chi^{(3)}\sim(\chi^{(1)})^4$ is used. From the refractive index dispersion we get $|\chi^{(3)}(\omega,\omega,\omega)|$ $=3.1\times10^{-14}$ esu at 1.064 μm. Using these values $|\chi_{xxxx}^{(3)}(\omega,\omega,\omega)|_{(CH)_x}$ can be determined.

IV. RESULTS AND DISCUSSION

A. $\chi^{(3)}(\omega,\omega,\omega)$ of polyacetylene

From the measurements described in the preceding section we obtained the following values for crystalline $trans$-$(CH)_x$:

$$|\chi_{xxxx}^{(3)}(\omega,\omega,\omega)|_{\lambda=1.064\ \mu m}=(9\pm4)\times10^{-9}\text{ esu },$$

$$|\chi_{xxxx}^{(3)}(\omega,\omega,\omega)|_{\lambda=1.907\ \mu m}=(1.7\pm0.7)\times10^{-8}\text{ esu }.$$

The uncertainty of these values arises from the error of

the sample thickness, the dielectric constants, the overall experimental error, and from some variations of the measured values at different positions on the sample. These are the largest reported values to date for an electronic $\chi^{(3)}$ inside the gap of any semiconductor. A comparison with some other organic and inorganic semiconductors and insulators is shown in Table I.[30,31] Polyacetylene has a third-order nonlinearity order of magnitude larger than any other semiconductor. As it can be seen from Table I, 1D semiconductors do not obey the generalized Miller's rule proposed by Wynne and Boyd,[32] which predicts a universal value of the ratio $\chi_{xxxx}^{(3)}/(\chi_{xx}^{(1)})^4$. The reasons for this strong deviation are the different polarization mechanisms responsible for the magnitudes of $\chi^{(1)}$ and $\chi^{(3)}$. Whereas $\chi^{(1)}$ is influenced by both the σ and π electrons, the contribution of the highly delocalized π electrons along the x axis to $\chi^{(3)}$ completely overwhelms that of the σ electrons. This characteristic feature is justified by our measurements: $\chi_{yyyy}^{(3)}$, $\chi_{xyyy}^{(3)}$, $\chi_{yxxx}^{(3)}$ turned out to be several orders of magnitude smaller than $\chi_{xxxx}^{(3)}$.

The electronic $\chi_{xxxx}^{(3)}$ of 1D semiconductors has been calculated by Agrawal et al.[33] within a one-electron theory using the tight-binding approximation. They give the expression for the off-resonance value of $\chi_{xxxx}^{(3)}$:

$$\chi_{xxxx}^{(3)}=\frac{32e^4a^3\sigma}{45\pi W^3}(W/E_g)^6 ,$$

where e is the electronic charge, $2a$ is the unit cell length along the chain direction (see Fig. 1), and σ is the density of the polymer chains. We take $W=12.8$ eV for the total width of the π bands from Ref. 34 and $E_g=1.5$ eV for the gap energy from Ref. 12. Furthermore, $2a=2.43$ Å and $\sigma=3.3\times10^{14}$ cm^{-2} after Ref. 11. With these numerical values we obtain $\chi_{xxxx}^{(3)}=3.2\times10^{-10}$ esu for $trans$-$(CH)_x$. A comparison with our results shows a discrepancy of almost 2 orders of magnitude between theory and experiment. There are some factors that may contribute to this deviation.

First, some resonance enhancement may be present in the measured values of $\chi_{xxxx}^{(3)}$. Secondly, local field corrections would slightly increase the theoretical value of the nonlinear susceptibility. However, even these two effects together cannot be made responsible for the large difference experienced between the theoretical and experimental results. We suggest that electron-electron interaction should be taken into account in the calculations of optical nonlinearities of polyacetylene. This conclusion is supported by recent electron-energy-loss spectroscopic studies on $trans$-$(CH)_x$.[34] From these measurements the ratio of the one-site electron correlation energy U to the total width of the π bands $U/4t_0\sim0.7$ is estimated. Thus, calculation of optical nonlinearities in polyacetylene (and probably also in other related 1D semiconductors) should be based on a Peierls-Hubbard Hamiltonian including the non-negligible electron repulsion energy U.[35]

B. The nonlinear index of polyacetylene

Sufficiently high light intensities give rise to an intensity-dependent change of the refractive index. The

nonlinear index n_2 relates the refractive index variation to the light intensity: $\Delta n = n_2 I$, and is linearly proportional to the real part of $\chi^{(3)}(\omega,-\omega,\omega)$. In contrast to the third-harmonic susceptibility, $\chi^{(3)}(\omega,-\omega,\omega)$ contains contributions from two different electronic processes. To identify these contributions, we recall the basic concept

for deriving the nonlinear susceptibilities. The solution of the equation of motion for the density matrix of the electronic system is obtained by successive approximation in ascending powers of the coherent periodic perturbation:[16,36]

$$-i\omega_k \rho^{(n)}(\omega_k) = -i\hbar^{-1}[H_0,\rho^{(n)}(\omega_k)] - i\hbar^{-1} \sum_{\substack{l,m \\ \omega_l+\omega_m=\omega_k}} [H_{\mathrm{coh}}(\omega_l),\rho^{(n-1)}(\omega_m)] + R\rho^{(n)}(\omega_k) \ ,$$

where H_0 is the time-independent Hamiltonian of the unperturbed system, H_{coh} is the interaction Hamiltonian describing the coherent perturbation by the incident radiation, R represents the damping constants, and $\rho^{(n)}(\omega_k) = \rho_k^{(n)} e^{-i\omega_k t}$ is the nth-order contribution to the density matrix. Thermodynamic equilibrium determines the components of $\rho^{(0)}$. For the nth order contribution to the polarization of the medium

$$\mathbf{P}^{(n)}(\omega_k) = \mathrm{Tr}[\rho^{(n)}(\omega_k)\mathbf{P}] \ .$$

Now, for $\rho^{(3)}(3\omega)$ there is only one possible combination of ω_l and ω_m with $\omega_l=\omega$ and $\omega_m=2\omega$ (ω denotes the angular frequency of the incident radiation). $\rho^{(3)}(\omega)$ and thus $\chi^{(3)}(\omega,-\omega,\omega)$, however, contain two components characterized by $\omega_l=\omega;\omega_m=0$, and $\omega_l=-\omega;\omega_m=2\omega$, respectively.

The first term in $\chi^{(3)}(\omega,-\omega,\omega)$ is due to change of the population distribution by absorption of the incident radiation. Consequently, the response time of this contribution is limited by the lifetime of the excited electrons τ. This relaxation time is much longer than the response time of the second contribution associated with distortion of the electronic states. The slow component becomes significant only near (one-photon) resonance (i.e., when the fundamental light gets absorbed). Under such resonant conditions the slow contribution depending on τ may exceed the fast one by several orders of magnitude.[37]

Recent transient photoinduced absorption and bleaching measurements[38] on crystalline trans-(CH)$_x$ enable us to deduce the slow contribution to $\chi^{(3)}(\omega,-\omega,\omega)$. For a fundamental beam at a wavelength of $\lambda=528$ nm polarized perpendicular to the chain direction we obtain the imaginary part of the slow contribution $\mathrm{Im}[\chi_{yyyy}^{(3)}(\omega,-\omega,\omega)_{\mathrm{sl}}]\sim 10^{-9}$ esu, which is a very high value for a lifetime as short as a few picoseconds. A Kramers-Kronig analysis yields a similarly large real part of this component. Comparing these results to those of similar investigations on unoriented samples,[39,40] we conclude that the ratio of $|\chi_{xxxx}^{(3)}(\omega,-\omega,\omega)_{\mathrm{sl}}|$ and $|\chi_{yyyy}^{(3)}(\omega,-\omega,\omega)_{\mathrm{sl}}|$ agrees fairly well with the ratio $\alpha_{xx}(\omega)/\alpha_{yy}(\omega)$, in agreement with the theory.

If the fundamental photon energy is considerably smaller than the gap energy, the slow contribution is negligible and the fast component becomes dominant in the expression for the nonlinear index. With neglect of dispersion: $\chi_{xxxx}^{(3)}(\omega,-\omega,\omega)_{\mathrm{fast}}\sim\chi_{xxxx}^{(3)}(\omega,\omega,\omega)$, and the

same relation applies for the y components. As a result, the fast contribution to the nonlinear index is strongly anisotropic due to the one-dimensional delocalization of π electrons, whereas the slow component appears to be considerably less affected by the one dimensionality of the electronic system. On the basis of the above considerations we can deduce the nonlinear index of polyacetylene in the optical gap from the measured values of $\chi_{xxxx}^{(3)}(\omega,\omega,\omega)$.

Assuming $\chi_{xxxx}^{(3)}(\omega,\omega,\omega)$ to be real, for light polarized parallel to the chain direction we obtain $n_2=(7\pm3)\times10^{-6}$ MW^{-1}cm^2 at $\lambda=1.064$ μm and $n_2=(2\pm0.8)\times10^{-5}$ MW^{-1}cm^2 at $\lambda=1.907$ μm. These impressing large values of the nonlinear index combined with a fast response time ($\sim10^{-15}$ s) and a high damage threshold (~50 GW/cm^2) in the near infrared region of the spectrum open attractive prospects for the use of this material in nonlinear optics. Nevertheless, the absorption is too high in the gap region for most applications. This residual absorption, which is mainly due to accidental doping by oxygen, can be reduced by orders of magnitude with compensation by NH$_3$. Such well transparent polyacetylene material may find important applications in the areas of optical bistability[41] and femtosecond optical pulse generation.[42,43]

V. SUMMARY

We have shown that strong dispersion of the linear optical constants near the band gap in semiconductors leads to interference between different driven harmonic waves in optical harmonic-generation measurements, provided that the sample thickness is smaller than the absorption length at the fundamental wavelength. This effect should be taken into account in the evaluation of harmonic-generation measurements in semiconductors under the conditions mentioned. We performed third-harmonic generation in crystalline trans-polyacetylene at two fundamental wavelengths in the gap region. A fused silica plate was used for calibration of the third-order susceptibility of polyacetylene. Air contribution to the third-harmonic signal was greatly reduced by choosing the confocal parameter of the fundamental beam much less than the coherence length of air.

The obtained values of the third-order susceptibility $\chi_{xxxx}^{(3)}(\omega,\omega,\omega)$ exceed by an order of magnitude those measured in the gap of other organic and inorganic semiconductors to date. The strong deviation of the mea-

sured values of $\chi^{(3)}_{xxxx}(\omega,\omega,\omega)$ from the prediction by a one-electron theory suggests the conclusion that electron-electron interaction may not be neglected in the calculation of nonlinear optical properties of polyacetylene. These and previous[38] measurements enable us to estimate the fast and slow electronic contribution to the nonlinear index of polyacetylene. The strongly different anisotropy of the two components is in agreement with theoretical considerations.

ACKNOWLEDGMENTS

*Permanent address: Institute of Physics, Technical University of Budapest, H-1521 Budapest, Hungary.

[1]J. P. Hermann, D. Ricard, and J. Ducuing, Appl. Phys. Lett. **23**, 178 (1973).

[2]K. C. Rustagi and J. Ducuing, Opt. Commun. **10**, 258 (1974).

[3]J. P. Hermann and J. Ducuing, J. Appl. Phys. **45**, 5100 (1974).

[4]J. Ducuing, in *Nonlinear Spectroscopy,* Proceedings of the International School of Physics "Enrico Fermi," Course LXIV, Varenna, 1975, edited by N. Bloembergen (North-Holland, Amsterdam, 1977).

[5]C. Sauteret, J. P. Hermann, R. Frey, F. Pradere, J. Ducuing, R. H. Baughman, and R. R. Chance, Phys. Rev. Lett. **36**, 956 (1976).

[6]H. Shirakawa, T. Ito, and S. Ikeda, Polym. J. **4**, 460 (1973).

[7]F. Kajzar, S. Etemad, G. L. Baker, and J. Messier, Solid State Commun. **63**, 1113 (1987).

[8]M. Sinclair, D. Moses, A. J. Heeger, K. Vilhelmsson, B. Valk, and M. Salour, Solid State Commun. **61**, 221 (1987).

[9]J. H. Edwards and W. J. Feast, Polym. Commun. **21**, 595 (1980).

[10]G. Leising, Polym. Bull. **11**, 401 (1984).

[11]H. Kahlert, O. Leitner, and G. Leising, Synth. Met. **17**, 467 (1987).

[12]G. Leising, Phys. Rev. B **38**, 10313 (1988).

[13]J. A. Armstrong, N. Bloembergen, J. Ducuing, and P. S. Pershan, Phys. Rev. **127**, 1918 (1962).

[14]N. Bloembergen and P. S. Pershan, Phys. Rev. **128**, 606 (1962).

[15]The complex amplitudes for the description of the fields are defined by their connection to the real (measurable) field strengths: $E^{real}(\mathbf{r},t)=E(\mathbf{r},t)+$c.c.

[16]We define nonlinear susceptibilities using the convention of Y. R. Shen, *The Principles of Nonlinear Optics* (Wiley, New York, 1984).

[17]J. Ducuing and N. Bloembergen, Phys. Rev. **133**, 1493 (1964).

[18]M. D. Levenson, C. Flytzanis, and N. Bloembergen, Phys. Rev. B **6**, 3962 (1972).

[19]E. Yablonovitch, C. Flytzanis, and N. Bloembergen, Phys. Rev. Lett. **29**, 865 (1972).

[20]G. R. Meredith, Phys. Rev. B **24**, 5522 (1981).

[21]*Handbook of Chemistry and Physics,* edited by R. C. Wearst and M. J. Astle (Chemical Rubber Company, Boca Raton, FL, 1982).

[22]C. L. Wang and E. L. Baardsen, Phys. Rev. **185**, 1079 (1969).

[23]J. F. Ward and G. H. C. New, Phys. Rev. **185**, 57 (1969).

[24]The value of $(\chi^{(3)})_A$ was taken as the average of the numbers reported in Refs. 22 and 23.

[25]*Handbook of Optical Constants of Solids,* edited by E. D. Palik (Academic, New York, 1985).

[26]G. R. Meredith, B. Buchalter, and C. Hanzlik, J. Chem. Phys. **78**, 1533 (1983).

[27]F. Kajzar and J. Messier, Phys. Rev. A **32**, 2352 (1985).

[28]F. Krausz and E. Wintner, Opt. Commun. (to be published).

[29]Our experimental procedure is in many aspects very similar to that used by D. Bethune, A. J. Schmidt, and Y. R. Shen, Phys. Rev. B **11**, 3867 (1975).

[30]P. Qiu and A. Penzkofer, Appl. Phys. B **45**, 225 (1988); instead of $\chi^{(3)}_{xxxx}$ an effective $\chi^{(3)}_{eff}$ governing THG under certain experimental conditions has been measured by the authors; this value is inserted in Table I.

[31]J. J. Wynne, Phys. Rev. **178**, 1295 (1969).

[32]J. J. Wynne and G. D. Boyd, Appl. Phys. Lett. **12**, 191 (1968).

[33]G. P. Agrawal, C. Cojan, and C. Flytzanis, Phys. Rev. B **17**, 776 (1978).

[34]J. Fink and G. Leising, Phys. Rev. B **34**, 5320 (1986).

[35]S. Mazumdar and S. N. Dixit, Phys. Rev. Lett. **51**, 292 (1983); J. E. Hirsch, *ibid.* **51**, 296 (1983).

[36]N. Bloembergen, *Nonlinear Optics* (Benjamin, New York, 1965).

[37]In indirect semiconductors (e.g., Si) with a long lifetime of the excited carriers $\chi^{(3)}_{xxxx}(\omega,-\omega,\omega)_{sl}$ may be as high as 10^{-5} esu. See, for example, R. K. Jain and M. B. Klein, Appl. Phys. Lett. **35**, 454 (1979).

[38]F. Krausz, P. Lasztity, J. S. Bakos, E. Wintner, and G. Leising, Appl. Phys. B **45**, 21 (1988).

[39]Z. Vardeny, J. Strait, D. Moses, T.-C. Chung, and A. J. Heeger, Phys. Rev. Lett. **49**, 1657 (1982).

[40]C. V. Shank, R. Yen, R. L. Fork, J. Orenstein, and G. L. Baker, Phys. Rev. Lett. **49**, 1660 (1982).

[41]To date, the slow electronic contribution and slow contributions of other types (e.g., thermal) to the nonlinear index have been preferred in the development of optically bistable elements for optical computing. See, for example, B. S. Wherrett, *Nonlinear Optics: Materials and Devices,* edited by C. Flytzanis and J. L. Oudar (Springer, Berlin, 1986), p. 180.

[42]H. A. Haus and Y. Silberberg, IEEE J. Quantum Electron. **QE-22**, 325 (1986).

[43]M. Yamashita, K. Torizuka, and T. Sato, Opt. Lett. **13**, 24 (1988).